Article

JOURNAL OF COMPOSITE MATERIALS

Journal of Composite Materials
2021, Vol. 55(13) 1769–1782

DOI: 10.1177/0021998320979037
journals.sagepub.com/home/jcm
SAGE

Investigation of the high temperature dry sliding wear behavior of graphene nanoplatelets reinforced aluminum matrix composites

Seçkin Martin[1], Sinan Kandemir[1] and Maksim Antonov[2]

Abstract

In this study, graphene nanoplatelets (GNPs) with a thickness of 50-100 nm have been utilized to improve the mechanical and tribological properties of A360 alloy due to their extraordinary mechanical properties and solid lubricant nature. For the investigation of tribological properties, ball-on disc tests were carried out at various temperatures including room temperature (RT), 150 °C, and 300 °C. According to the hardness and ball-on-disc test results, the nanocomposite samples reinforced with GNPs exhibited improved hardness and wear resistance. The improvement in the wear behavior of nanocomposites was referred to the temporarily formed solid lubricant film of harder GNPs during the wear, and hence coefficient of friction (COF) and volume loss were considerably reduced. Abrasive-adhesive, oxidative, and mild-to-severe were found to be main wear mechanisms at RT, 150 °C, and 300 °C, respectively. Overall, the results show that the nanocomposites fabricated by casting method combined with mechanical stirring and ultrasonication have promising wear performance, especially at elevated temperatures. This may suggest that these developed materials could be potential candidates to be used in the engineering applications requiring high temperature wear performance.

Keywords

Graphene nanoplatelet, metal matrix nanocomposite, dry sliding, elevated temperature, microstructure

Introduction

Owing to their high specific strength, high specific modulus and low density, aluminum (Al) and its alloys are broadly employed in the automotive and aerospace industries to reduce weight, hence energy consumption and CO_2 emission.[1,2] Despite improved mechanical properties of Al alloys, the majority of these alloys suffer from their low hardness and wear resistance at elevated temperatures. The use of suitable lubricants between contact surfaces is one of the widely applied solutions to deal with the wear phenomenon, but reduction in coefficient of friction (COF) and volume loss may not be achieved under challenging conditions, such as high temperature and high pressure.[3] Therefore, many efforts have been devoted to improve wear resistance of Al alloys, these include introduction of proper reinforcing materials into alloys and surface coating applications in order to meet the requirements in specific engineering application.[4,5] Numerous research studies have shown that the addition of micron-sized discontinuous reinforcements into Al matrix by a suitable mixing technique significantly enhanced the wear resistance of monolithic alloys.[6–8] However, unlike the strength and wear resistance, the ductility generally tends to decrease in these composites due to considerable brittle reinforcement content. This limitation hampers the use of such wear resistant composites with micron-sized reinforcement in broad engineering application areas. On the other hand, several studies[9–15] revealed that the addition of

[1]Faculty of Engineering, Department of Mechanical Engineering, Izmir Institute of Technology, Turkey
[2]Department of Mechanical and Industrial Engineering, Tallinn University of Technology, Estonia

Corresponding author:
Sinan Kandemir, Faculty of Engineering, Department of Mechanical Engineering, Izmir Institute of Technology, Gulbahce 35430 Urla, Izmir, Turkey.
Email: sinankandemir@iyte.edu.tr

nano-sized ceramic and/or carbon (C)-based reinforcements increased strength and wear resistance of metal matrices by promoting effective stress transfer and grain refinement. Graphene has been widely considered to be one of the promising and attractive reinforcements for different matrices including polymers following its synthesis in 2004 due to its outstanding physical and mechanical properties.[16,17] In addition, due to the weak van der Waals bonds, layered structure of graphene nanoplatelets (GNPs) which consist of several layers of graphene could be sheared easily, and hence it can be expected that the incorporation of GNPs into metals exhibits a solid lubrication effect on contact surfaces to reduce friction and consequently wear.[18] Moreover, graphene layers could reduce volume loss and prevent the cracks which may take place during sliding by acting as barriers to crack propagation.[19–21]

There are several investigations reported in the literature regarding the introduction of GNPs into metals in order to improve their mechanical and/or tribological performance.[22–24] GNPs were commonly incorporated into such matrices by means of powder metallurgy which is thought to be an effective technique in terms of obtaining a uniform dispersion of finer reinforcements through matrix. Tabandeh-Khorshid et al.[22] investigated the effect of GNPs on the tribological properties of Al matrix nanocomposites produced by powder metallurgy. The results showed that 0.1 wt.% GNP addition exhibited better wear resistance than unreinforced Al and the composite reinforced with 1 wt. % GNP. In addition, the highest wear rate was observed in the sample with 1 wt.% GNP. This result can be attributed to the formation of GNP clusters formed due to relatively high content of GNPs in the matrix, which induced a significant volume loss during sliding in the wear test. El-Ghazaly et al.[25] reported that the wear rate of Al/GNP (3 and 5 wt.%) nanocomposites fabricated by a combination of ball milling and hot extrusion process decreased compared to that of unreinforced Al alloy. However, the composite containing 3 wt.% GNP displayed lower COF value and greater wear resistance than those of the composite with 5 wt.% GNP. This result suggests that during the sliding a temporary protective interlayer could not be formed on the contact surface due to the potential agglomeration of relatively high amount of GNPs in Al/5 wt.% GNP samples.

Besides powder metallurgy, casting is one of the most frequently preferred fabrication techniques by the industry in terms of providing relatively scalability, simplicity, and low-cost.[26] However, it is evident from the published studies that only a few attempts on the production of GNP reinforced Al matrix nanocomposites by liquid state routes were made to date.[27,28] Like other nano-sized reinforcement types, poor wettability, high surface-to-volume ratio and thus agglomeration tendency of GNPs are regarded as the main barriers for their uniform dispersion into molten metals to achieve good interfacial bonding and hence enhanced mechanical properties. In these cases, the introduction of high intensity ultrasonic waves into melt, namely ultrasonic mixing of GNPs, and/or the use of partial powder metallurgy in the process are the most frequently referred approaches to facilitate deagglomeration of GNPs.

It is crucial to understand friction and wear behaviors of engineering components operating at elevated temperatures, such as piston-cylinder system and turbine parts since strength of materials is significantly reduced and adhesion characteristics of contact surfaces is altered with increasing temperature. Consequently, applications involving high temperatures may show completely different wear mechanism resulting in serious wear rates. In this regard, according to the best of our knowledge, there is no available data associated with the investigation of high temperature wear behavior of GNP reinforced Al matrix nanocomposites fabricated by solidification processes in the literature. It is therefore aimed at investigating the influence of GNP additions on both ambient and high temperature dry sliding wear characteristics of composites which are fabricated by means of a combination of stir casting and ultrasonic mixing in the present work. Along with the detailed microstructural analyses, the wear mechanisms in the fabricated samples are also explored and discussed based on the worn surface observations.

Experimental

In this work, A360 (Aluminum Association Designation) commercial aluminum, one of the widely used alloys in industry, was used as the matrix material and its chemical composition is given in Table 1. Since silicon (Si) imparts castability to the alloy, the presence of relatively high Si content in the alloy can be beneficial for the ease of composite casting. Another aspect of choosing A360 alloy is the potential of its higher Si content to suppress the reaction between Al and GNPs, which forms undesirable Al_4C_3 phase at the matrix-reinforcement interface. Thus, a strong bonding and hence improved mechanical properties can be achieved. GNPs which have an average thickness of 50-100 nm and diameter of 5 μm

Table 1. Chemical composition of A360 alloy (wt.%).

Al	Si	Fe	Cu	Mn	Mg	Zn	Ti
Bal.	10.0	0.5	0.10	0.50	0.35	0.10	0.15

were used as the reinforcement. The scanning electron microscopy (SEM) images of the GNPs are shown in Figure 1.

GNPs were not directly fed into the matrix in order to prevent them from floating due to the oxide layer formed on the melt surface in spite of using protective gas. They were introduced into the liquid matrix with Al powders in the form of master alloys (tablets). Prior to the casting process, the ball milling (Retsch PM 200) operation was performed for 2 h at 350 rpm to blend the Al and magnesium (Mg) powders along with GNPs. The purpose of incorporating Mg powders was to reduce the relatively high surface tension of A360 alloy. During the ball milling operation, stainless steel balls were used with a ball to powder ratio of 9:1. The Al and Mg powders with an average size of $\leq$75 μm and purity of 99% were utilized for the deagglomeration of GNPs. After the ball milling process, the mixture was cold pressed into 30 mm diameter tablets under 250 MPa.

The experimental arrangement for composite fabrication is shown schematically in Figure 2. Once approximately 200 g A360 alloy was melted in a graphite crucible by an electric resistance furnace at 700 °C, the tablet feeding process was launched. During the feeding, mechanical stirring was applied for 15 min. at 400 rpm in order to facilitate the erosion (fragmentation) of tablets and hence the distribution of GNPs throughout the matrix. Then, 15 min. ultrasonic treatment was applied to the liquid composite at 675 °C by an ultrasonic device (Q700-Qsonica, LLC with 12.7 mm diameter grade 5 titanium probe and power output of 700 W) in order to obtain homogeneous reinforcement distribution and dispersion. After sonication, the liquid composite was cast into a pre-heated permanent steel mold at around 300 °C. The GNP contents in composites were set to be about 0.25 and 0.5 wt.% for different sets of samples. The reference alloy without the addition of GNPs was also prepared with the same method followed for the nanocomposite fabrication to observe any potential individual effect of GNPs on the matrix.

The samples were ground and polished up to 1 μm surface finish with traditional metallographic sample preparation steps for microstructural analysis. An optical microscope (Leica DM2500 M) and SEM (FEI Quanta FEG 250) fitted with an energy dispersive X-ray spectroscopy (EDX) were utilized to examine the microstructures. Transmission electron microscope (TEM, FEI Tecnai F30 with an EDX system) with an operating voltage of 200 kV was also used to observe the reinforcement-matrix interface. For TEM sample preparation, an ultramicrotome device (Leica EM UC6) was employed by sectioning the composite into very thin electron transparent layers. The average grain sizes of samples were determined according the linear intercept method (ASTM E112 standards). Vickers hardness (HV) tests were performed based on ASTM E92-82 standards under a load of 1 kgf and 10 s dwell time. At least ten indentations were made on each sample and the average data was reported.

In order to investigate the dry sliding wear behavior of reference alloy and composites, the specimens were machined from the cast blocks into 15 mm diameter and 7 mm height discs. The disc surfaces which will be exposed to the contact were then ground and polished down to 1 μm finish. The ball-on-disc tests were conducted three times for each case against the AISI 52100 steel ball (62 HRC) in 10 mm diameter by a tribometer (CETR-Bruker UMT-2 model equipped with S21ME1000 lower rotary drive, DFH-20 dual friction/load sensors and suspension for load of 200 N and 30 N, respectively.), as schematically shown in Figure 3, at various temperatures, i.e. RT, 150 °C and 300 °C.

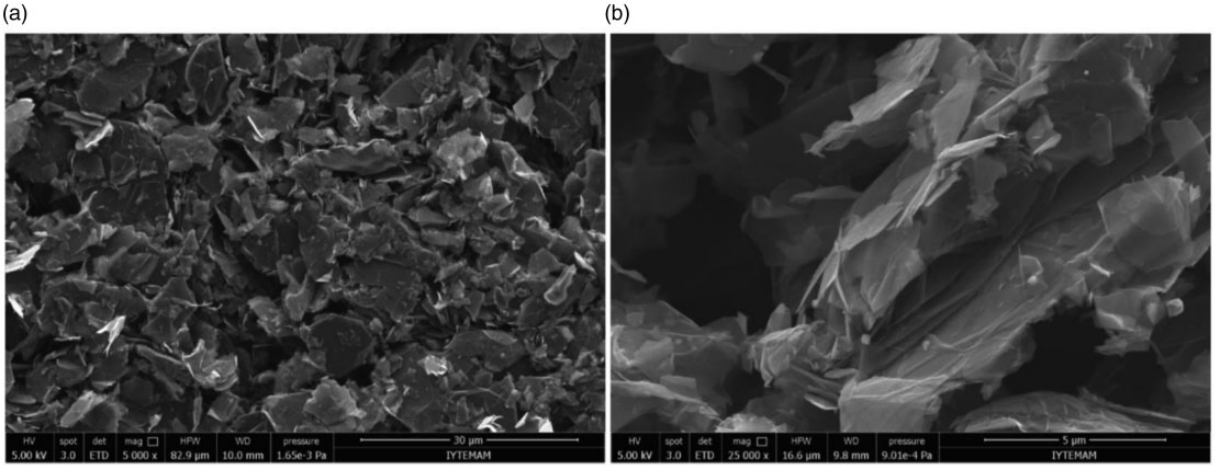

Figure 1. a) Low and b) high magnification SEM images of the GNPs used in this study.

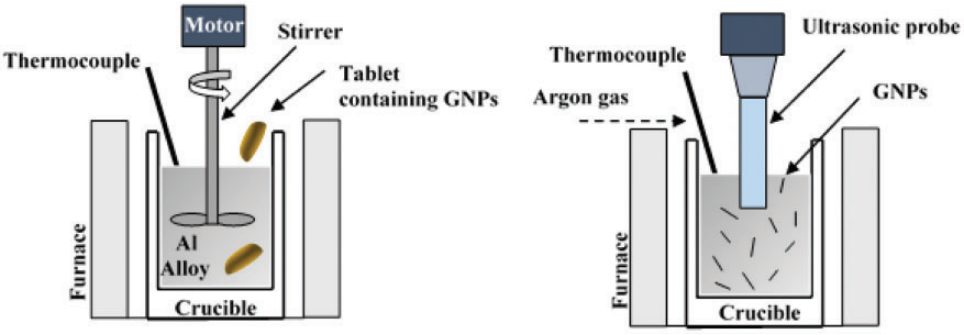

Figure 2. Scheme of the experimental arrangement for the fabrication of GNP reinforced Al nanocomposites.

It is considered that working in these temperature ranges can provide the similar tribological conditions that the majority of Al alloys will show in high temperature applications. Thus, the obtained test results are most likely to be comparable to those of real cases. The wear test parameters are given in Table 2. The Hertz contact stress was estimated to be around 380 MPa which is nearly equal to the compressive strength of reference alloy. For this reason, the ball-on-disc test was designed in three steps: track generation, check run, and long period (real test) with a total sliding distance of 1000 m and 7 mm track diameter. The track generation step was done to shift conditions from point to elliptical contact being closer to those occurring in ball, sliding bearings and other sliding contacts. The sample surface was lubricated with unmodified (without additives) oil (ExxonMobil SpectraSyn 8) to generate a smooth surface. After this stage, the lubricant was immediately washed out with acetone and ethanol. In the second step, check run, the sample was worn for a short period of time prior to long-term test in order to observe any problems related to the samples such as premature failure due to the presence of micron-sized pores. In addition, testing of aluminum alloys is sometimes associated with significant vibrations, and check run is required to assess the state of device (especially that of force sensor). After performing three wear tests for type of material and condition, the volume losses were calculated with the help of 3 D laser scanning machine (Bruker Contour GT-K) and their average values were presented along with COF results.

Results and discussion

Figures 4 and 5 show the optical micrographs and average grain sizes of reference alloy and composites, respectively. As seen, the introduction of GNPs into the matrix partially inhibited the growth of dendrites that were already available in the A360 alloy as primary α-Al grains (Figure 4(a)), leading to a limited grain refinement. Although several mechanisms have been proposed for grain size reduction by the addition of reinforcement, the mechanism in this case is more likely to be the fact that the GNPs act as nucleating agents during solidification of α-Al. In addition, when the GNP content increased from 0.25 to 0.5 wt.%, the grain size refinement potency is weakened presumably due to the clustering tendency and non-uniform dispersion of relatively high amount of reinforcements.

As seen in Figure 6, the SEM micrographs of composites show relatively homogeneous dispersion and distribution of potential GNPs into the matrix, suggesting that the ball milling process used prior to the composite fabrication as well as ultrasonication may have played a substantial role in terms of deagglomeration of GNPs. Despite the effective distribution of reinforcement throughout A360 alloy, it seems that some GNP clusters still exist in the microstructures, particularly in those of the composite with 0.5 wt.% GNP (Figure 6(b)). For example, such a potential GNP cluster with the point EDX analysis is shown for the A360/0.25 wt.% GNP composite in Figure 7. The significant C concentrations in the analysis are most likely to indicate the presence of GNPs in that location of Al matrix. It can be also noticed from Figure 7 that the size of GNPs incorporated into the produced sample is smaller than the size of as-received GNPs. This may be due to the fracture of GNPs during the ball milling process. It can be suggested that in several locations of the A360/0.5 wt.% GNP composite the GNPs may appear as relatively larger clusters or agglomerates as illustrated in the EDX elemental mapping in Figure 8. This observation implies that increasing GNP content is likely to further complicate its distribution into the matrix. Also, such agglomerates can be expected to result in a reduction in the mechanical properties and high volume loss in the wear tests due to effortless detachment of comparatively porous GNP agglomerations from the alloy.

The TEM images and EDX analysis of the composite with 0.25 wt.% GNP prove that the GNPs were randomly embedded into the matrix, showing no

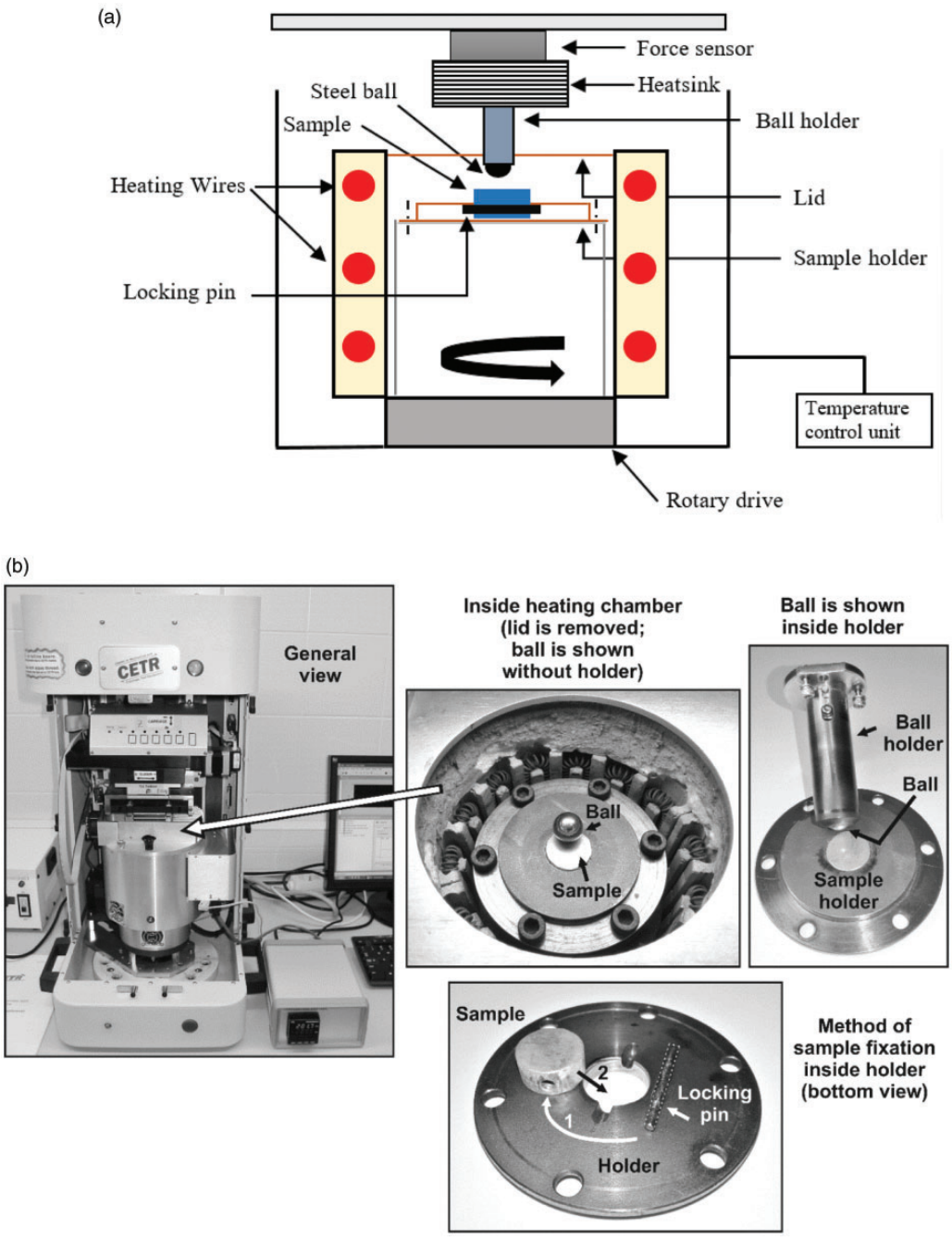

Figure 3. (a) Schematic illustration of ball-on-disc mode wear test at elevated temperatures, and (b) pictures and arrangement of the tribometer device used in the present work.

Table 2. Parameters of ball-on-disc test.

Steps	Load (N)	Duration (min.)	Speed (rpm)	Temperature (°C)
Track Generation	20	1	1	RT / 150 / 300
Check run	2	1	273	RT / 150 / 300
Real test	2	83	273	RT / 150 / 300

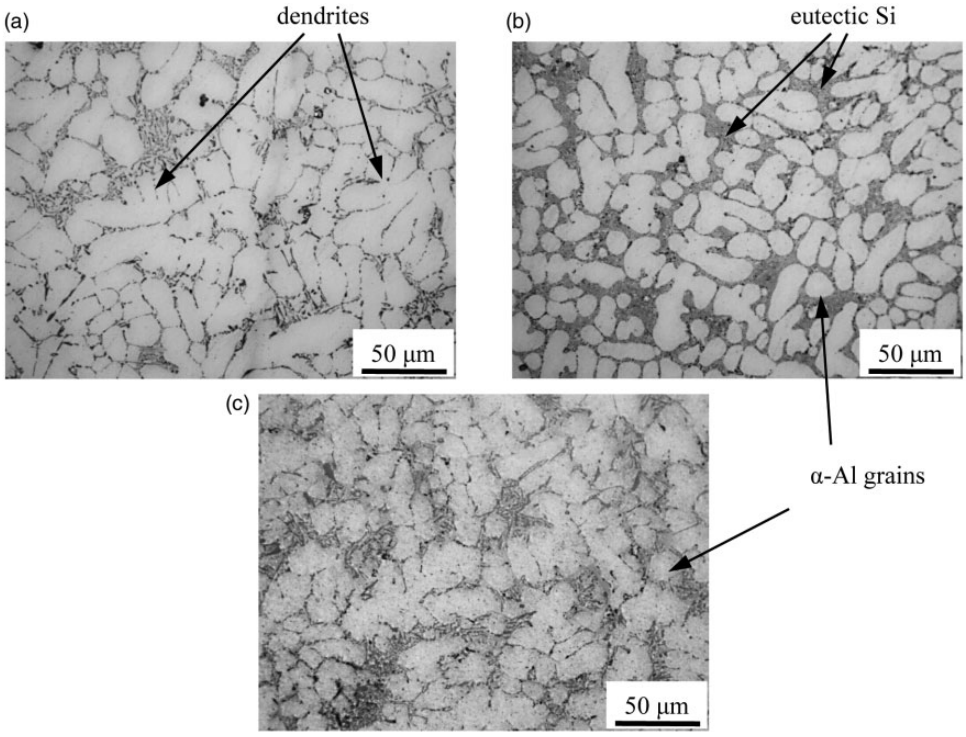

Figure 4. Optical micrographs of (a) A360 reference alloy, (b) A360/0.25 wt.%GNP and (c) A360/0.5 wt.%GNP composites.

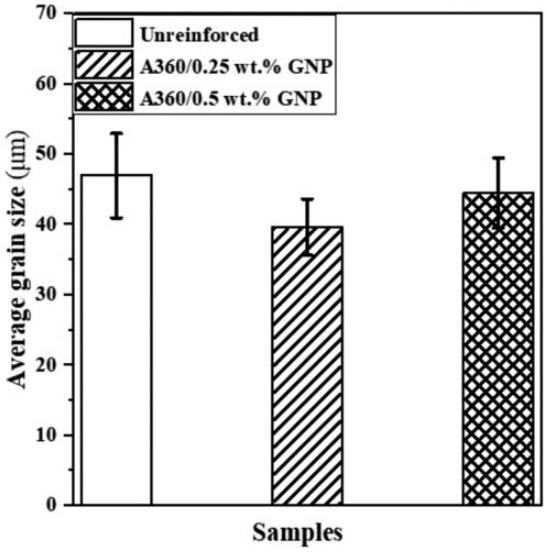

Figure 5. Average grain sizes of the unreinforced alloy and the composites with 0.25 wt.% and 0.5 wt.% GNPs at ambient temperature.

preferential orientation, as indicated in Figures 9 and 10. The horizontally and vertically oriented GNPs are displayed in Figure 9(a) and (b), respectively. Figure 10 presents the areal EDX analyses for the various locations marked in Figure 9(a). The presence of GNPs in the matrix can be also verified by the measured interplanar distance of 0.34 nm which is consistent with the literature[29] (Figure 9(b)). As seen, there is no detectable void or additional phase at the reinforcement-matrix interface, which may infer that a clean bonding was achieved for effective load transfer. This clean bonding can be attributed to the relatively high level of Si content with at least 10 wt.% in the vicinity of reinforcement to prevent any chemical attack between the GNPs and Al matrix as stated earlier (see the Si peak in Figure 10(c)).[30]

Figure 11 shows the average hardness values of reference alloy and composites at ambient conditions. It is clear that the GNP reinforced samples exhibited enhanced hardness results compared to the reference alloy due to harder nature and grain refining effect of GNPs. Figure 12(a) compares the average COF values obtained from the ball-on-disc wear tests of all samples at the indicated test temperatures. As seen, despite the divergent COF outcomes for all samples, the composite containing 0.25 wt.% GNP reached the minimal average COF values among the others over the whole temperature range, indicating the solid lubricant effect of effectively distributed GNPs on the matrix surface (see Figure 7).[18] Besides, the composite with 0.5 wt.% GNP showed considerably higher COF values which deviated over a very narrow band compared to those of the composite with 0.25 at all test temperatures.

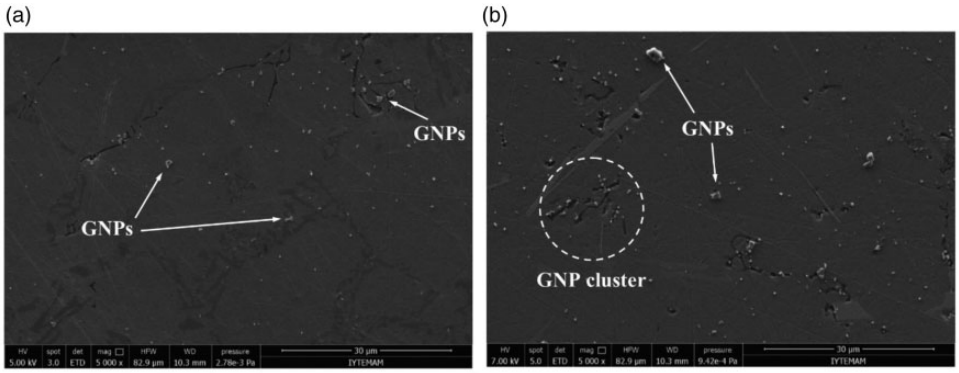

Figure 6. Secondary electron SEM images of (a) A360/0.25 wt.%GNP and (b) A360/0.5 wt.%GNP cast composites showing potential GNP sites.

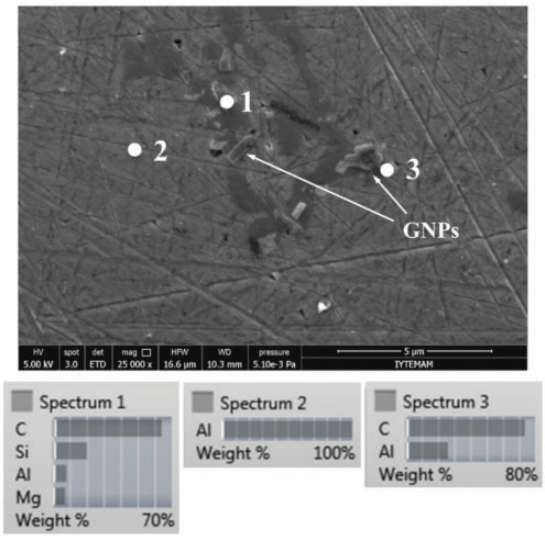

Figure 7. Point EDX analysis for a region in A360/0.25 wt.% GNP composite.

This circumstance can be obviously explained by the agglomeration and non-uniform dispersion of GNPs throughout the composite (see Figure 8). It is also spotted that the COF result for the reference alloy sharply increased at the highest test temperature (300 °C), which is most likely to be due to a dramatic increase in the ductility with increasing temperature, hence resulting larger contact area under the load, in the absence of reinforcement.

Figure 12(b) reveals the influence of GNP contents and temperature on the wear loses of the alloy discs. It seems that the samples exhibited comparable trends for both COF and wear loss results at all conditions, verifying the close relation between friction and wear. In other words, both friction and wear outcomes having intermediate levels at RT went through a minimum at 150 °C and then reached to their maximum values at 300 °C for all samples with only one exception as A360/0.5 wt.% GNP composite displayed very similar COF data at all test temperatures. This trend could suggest that there is a change in the wear regime between 150 °C and 300 °C. At ambient condition, the A360/0.25 wt.% GNP composite possessed a significant decrease in the wear loss by 40%, while the A360/0.5 wt.% GNP composite showed about 25% wear loss increment compared to that of reference alloy after 1000 m sliding distance. The enhancement in wear resistance by 0.25 wt.% reinforcement content is ascribed to the effective distribution of harder GNPs into the alloy. This is corresponded to the hardness test results as hardness is well known to be one of the parameters affecting the wear rate based on the Archard equation ($Q = KW/H$, where Q is the total worn volume per unit distance, K is the coefficient of wear, W is the total normal load and H is the indentation hardness).[31] However, there is a discrepancy between the hardness test and calculated volume loss results of reference alloy and composite with 0.5 wt.% GNP. This is presumably related to the ease of GNP clusters fragmentation from the composite surface with increasing GNP contents. Also, there could be more available individual GNPs on the contact surface of alloy with 0.25 wt.% GNP compared to 0.5 wt.% GNP content. It is considered that the potential GNPs of A360/0.5 wt.% GNP sample could not be released and not effectively cover the contact surface as a solid lubricant during sliding due to the lack of homogeneity.[32,33] In other words, there might be a positive effect of GNPs in some areas of that sample, but damage initiated in areas where GNPs tend to form conglomerates leads to overall reduction in the wear resistance. Therefore, A360/0.25 wt.% GNP samples exhibit better wear resistance than A360/0.5 wt.% GNP. As temperature increases to 150 °C, the wear

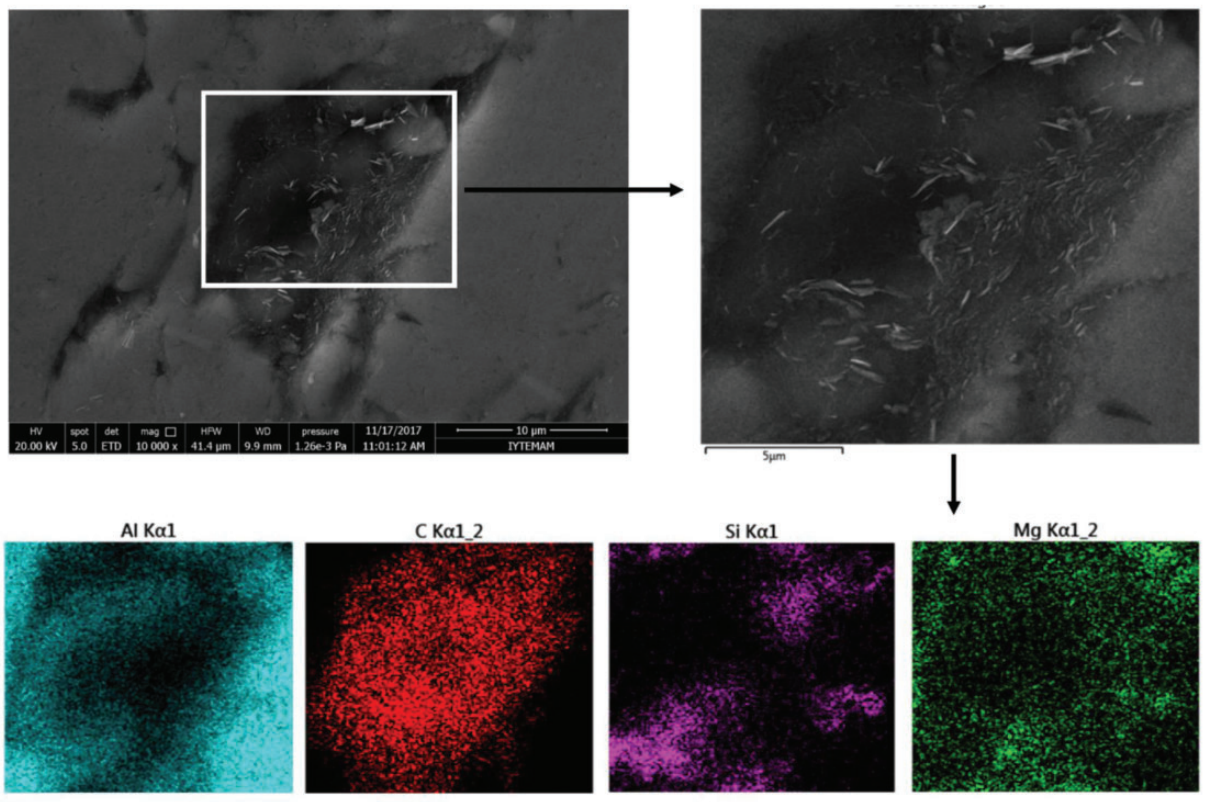

Figure 8. EDX elemental mapping for a region in A360/0.5 wt.% GNP composite.

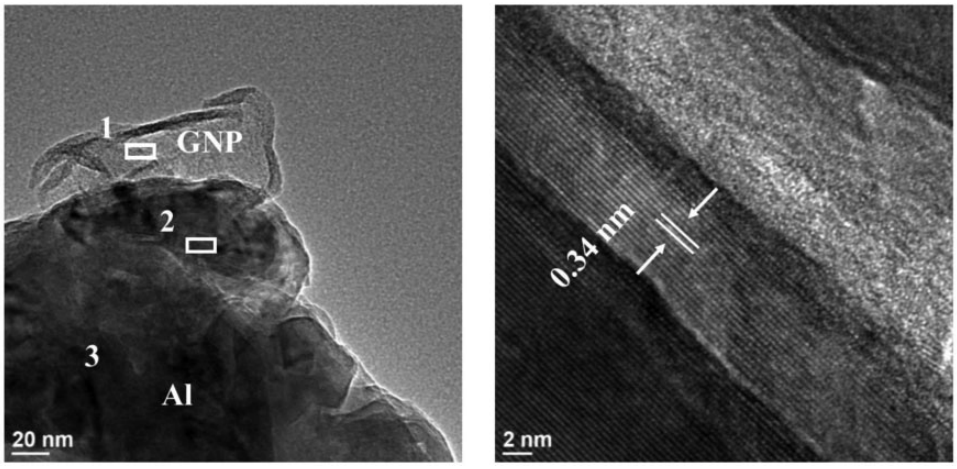

Figure 9. TEM images of (a) horizontally and (b) vertically embedded individual GNPs into A360/0.25 wt.% GNP nanocomposite.

loses decrease for all samples and the A360/0.5 wt.% GNP composite still exhibits the highest wear loss. In addition, the wear loss difference between the unreinforced alloy and A360/0.25 wt.%GNP composite became negligible at 150 °C.

The representative 3 D scanned surfaces for all samples after the wear tests conducted at various temperatures were given in Figure 13 in order to correlate them with the volume loss data. When the scales were evaluated at RT, relatively deeper wear scar zones were observed in the unreinforced alloy as indicated in Figure 13(a). On the other hand, A360/0.5 wt.%GNP sample displayed a broader wear scar at ambient condition compared to the composite with 0.25 wt.% GNP (Figure 13(b) and (c)). At 150 °C, it seems that the A360/0.25 wt.%GNP sample has the shallowest and

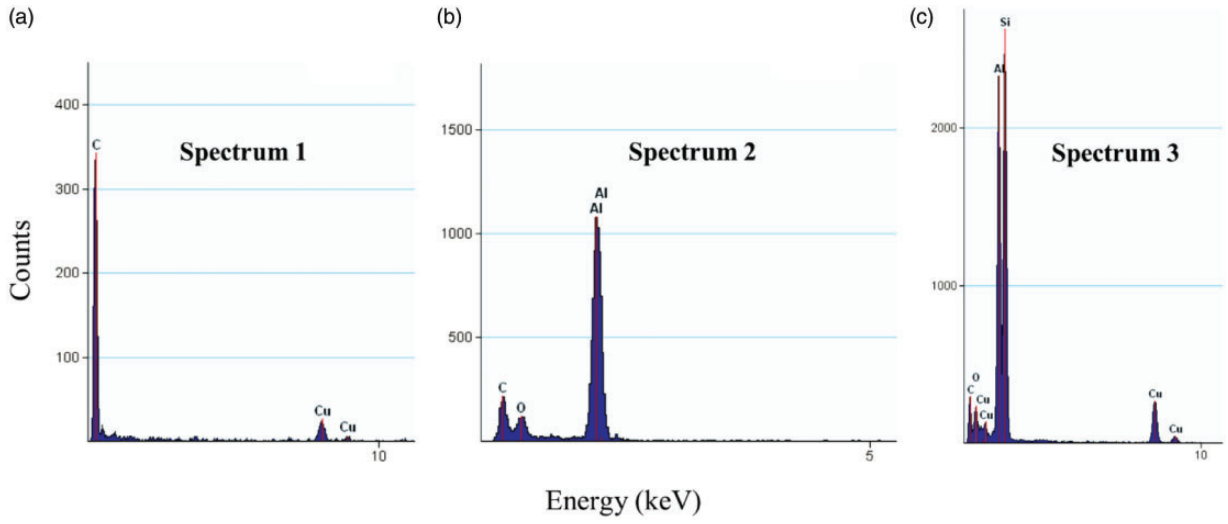

Figure 10. EDX results of the locations marked in Figure 9 for A360/0.25 wt.% GNP nanocomposite.

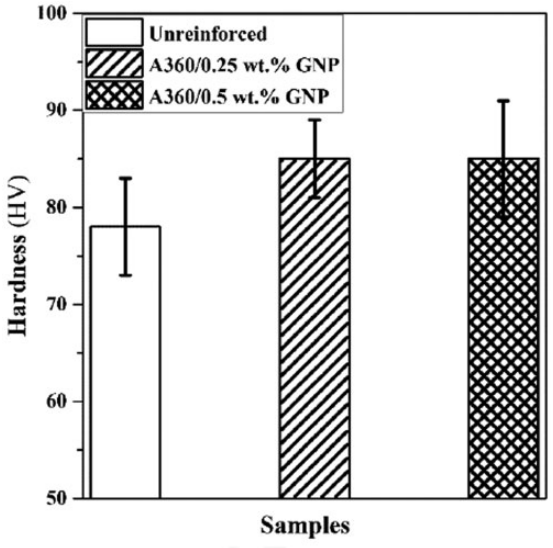

Figure 11. Average hardness values of A360 alloy and its composites with 0.25 and 0.5 wt.% GNPs at RT.

narrowest wear scar among the other samples as shown in Figure 13(e) (note that the color scale bars indicating the depth level vary from sample to sample). It could be suggested that considerable softening of the matrix at 300 °C led to uneven and catastrophic wear scars for the reference alloy and nanocomposites compared to the other worn surfaces (Figure 13(g) to (i)). However, the composite containing 0.25 wt.% GNP displayed relatively lower wear depth.

Figure 14 reveals the SEM micrographs for the surfaces of unreinforced and GNP reinforced Al alloy discs after the wear tests at RT, 150 °C and 300 °C. The scratch marks which were oriented parallel to the sliding direction can be directly identified from the worn surfaces at RT (Figure 14(a) to (c)). Fine grooves and ploughing marks indicate the abrasive wear that is more likely to be predominant wear mechanisms during the tests.[34–35] Additionally, the presence of delamination patches on all worn sample surfaces may imply that adhesive wear mechanism operated as well. A360/0.25 wt.%GNP sample can be easily distinguished from the others as it has relatively smoother worn surface due to the lubricious effect of GNPs, which is consistent with the volume loss results (see

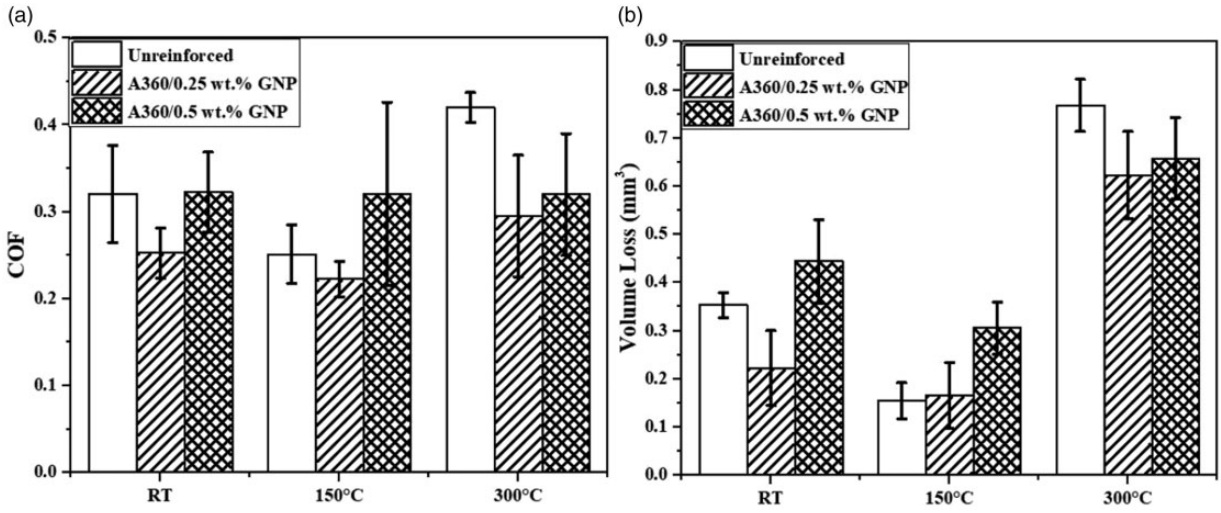

Figure 12. Comparison of (a) the COF and (b) volume loss values of the alloys depending on GNP contents and wear test temperatures.

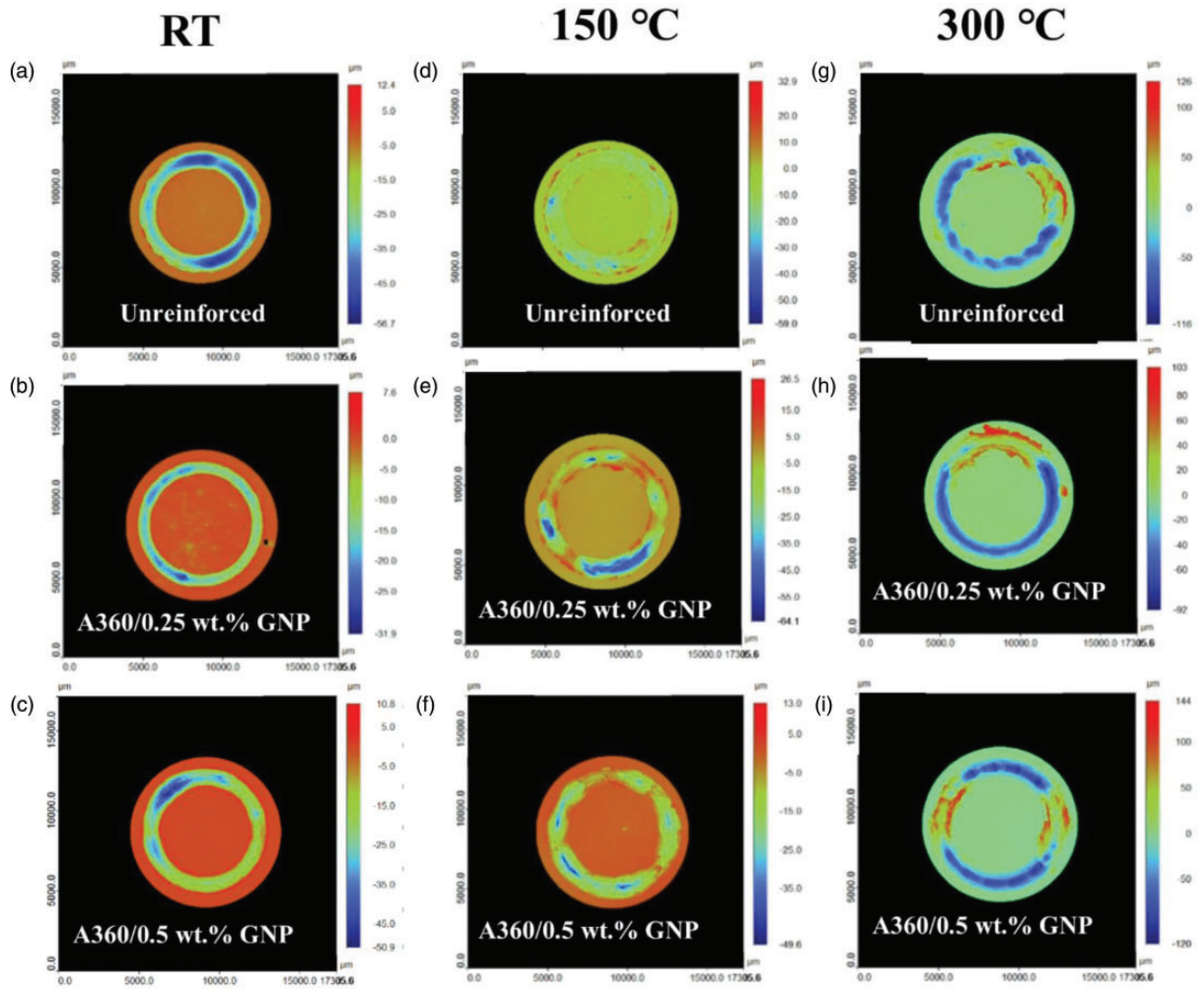

Figure 13. 3 D scanned surfaces of the reference alloy and nanocomposite discs worn at indicated temperatures.

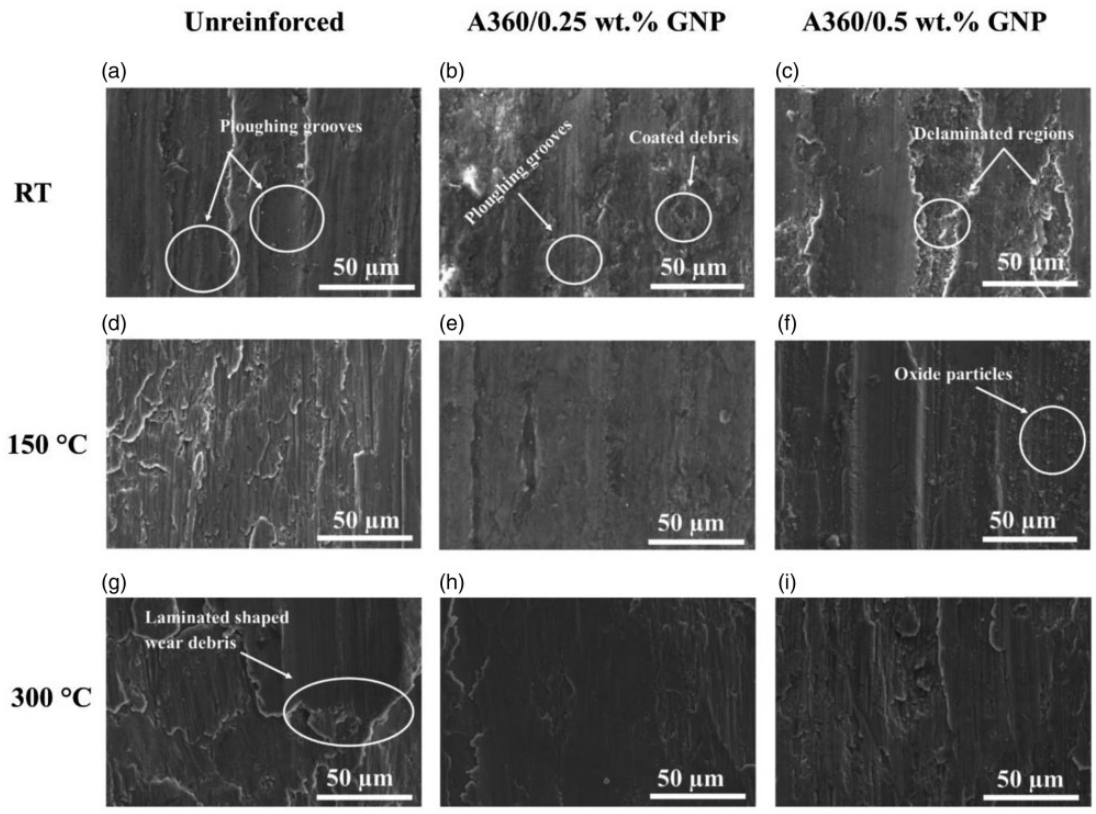

Figure 14. SEM micrographs taken from the center of wear scars in the surfaces of reference alloy and nanocomposite discs after ball-on-disc wear tests at indicated temperatures.

Figure 12(b)). The presence of GNPs on the worn surfaces can be seen in Figure 15 for the 0.25 wt.% GNP reinforced disc tested at RT.

The wear particles can be spotted on the sample surfaces worn at 150 °C, as evidently shown in Figure 14(f). The EDX analysis performed on such a particle rich area contains high level of oxygen, indicating the significant oxide formation due to increased oxidation rate at elevated temperatures (Figure 16). It is considered that the surfaces of composites were covered with oxide films to some extent with the inclusions of GNPs, which is supported by the C content in the EDX analysis. During sliding, it is argued that such oxidized particles (resulting in formation of aluminum oxide) entrapped between the mating surfaces may serve as abradants for three-body abrasion or be integrated into a surface to operate as two-body abrasion.[36–37] It can be therefore suggested that the dominant oxide particles could prevent the direct contact between the softer matrix and steel counterface leading to a reduction in the wear loses for all samples at 150 °C. During the sliding process, it is also possible that the freely moving oxide particles are accumulated on the wear tracks, and the wear debris containing these oxide particles are consequently compacted as a result of compressive load to temporary form a load-bearing layer.[38–40] Such a partially formed protective layer contributing to the wear resistance is given as a potential example in Figure 17 for the A360/0.25 wt.%GNP composite. Along with the reduction in the wear loses, the noticeable drop of COF values in the reference alloy and A360/0.25 wt.%GNP composite discs tested in comparison with the room temperature data could be also attributed to the self-lubricating effect of the oxide layers formed at 150 °C.[41]

It has been reported that the mechanical properties of tribo-couples must be taken into account along with the oxidation phenomena in order to document the acting wear mechanisms at higher temperatures.[42] It is known that Al-Si alloys are significantly softened when temperature exceeds 250 °C.[35] Therefore, the protective oxide layer is unlikely to remain stable on the surfaces worn at 300 °C due to the large amount of plastic deformation of matrix, leading to continuous fracturing of insufficiently supported oxide layers. Then, the broken oxide layers can work as abrasive particles. This suggests that the wear mechanism was transformed from mild to severe wear, which can be characterized by the laminated-shaped wear debris on the worn surfaces as indicated in Figure 14(g).

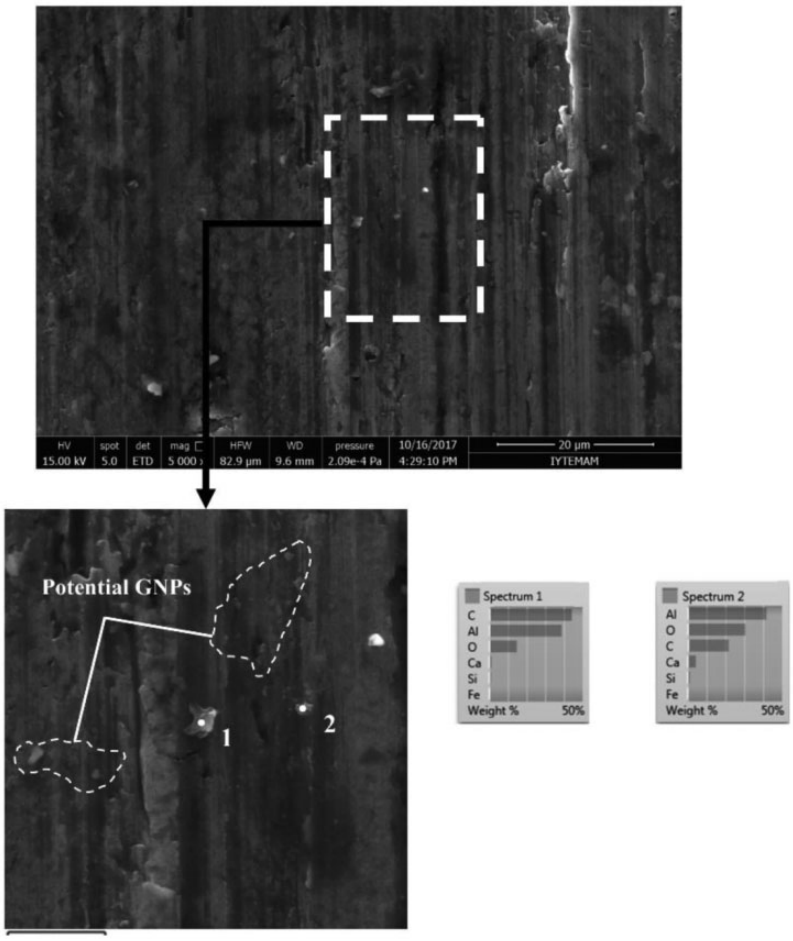

Figure 15. SEM micrograph and EDX analysis of wear scar in the surface of A360/0.25 wt.%GNP composite disc after the wear test at RT.

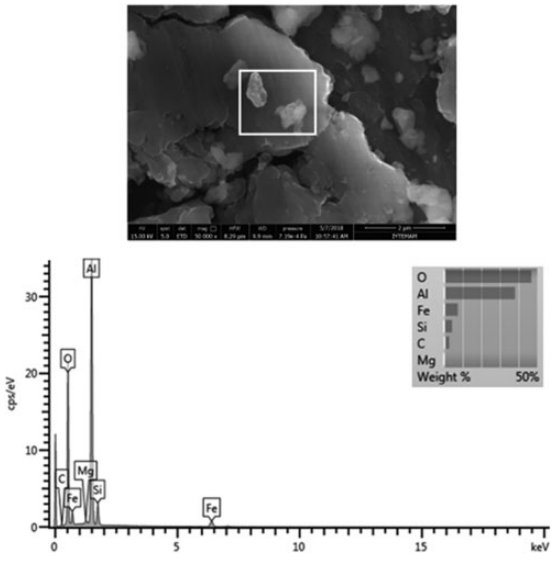

Figure 16. EDX analysis of the wear debris found on the A360/0.5 wt.%GNP composite disc (Figure 14f) after the wear test at 150 °C.

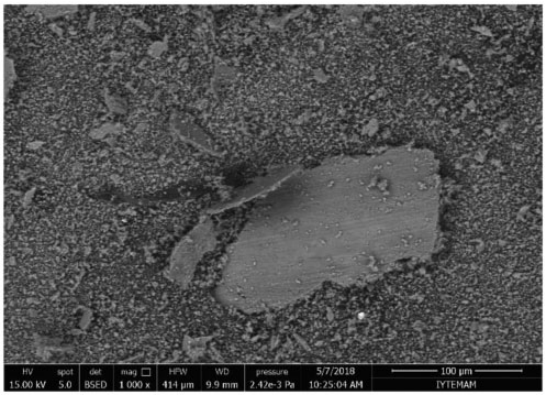

Figure 17. Wear debris showing formed oxide protective layer on the A360/0.25 wt.%GNP composite disc (Figure 14f) after the wear test at 150 °C.

Conclusions

In the present study, the effect of 0.25 and 0.5 wt.% GNPs additions on the microstructure, room and

high temperature friction and wear behaviors of A360 alloy has been investigated. Based on the experimental works, the following conclusions can be drawn:

1. The stir casting combined with the application of ultrasounds has been found to be a promising approach in terms of obtaining effective reinforcement distribution throughout the matrix.
2. The electron microscopy images showed that a more uniform dispersion and distribution of GNPs was achieved for the 0.25 wt.% content rather than 0.5 wt.% GNP addition. No void or secondary phase between the matrix and GNPs was detected, suggesting that a clean bonding, hence effective load transfer, was obtained.
3. At room temperature, 0.25 wt.% GNP addition into A360 alloy resulted in a significant reduction in both COF and wear loss compared to the reference alloy due to the grain refining (hardening) and solid lubrication impacts of GNPs. At 150°C, almost every sample exhibited an enhancement in the friction and wear resistance compared to their performance at RT due to the formation of protective oxide layer with sufficient support of base metal at elevated temperatures and self-lubricating effect of GNPs. A sharp increase in the COF and wear loss values was observed for the reference and composite discs at 300°C as a result of considerable softening of Al and inability of the matrix to provide an adequate support formed oxide layer.
4. Due to the presence of ploughing grooves and delamination patches, abrasive and adhesive mechanisms were suggested to be the main mechanism at RT. While the dominant wear mechanism at 150°C was the oxidation wear based on the detected oxidized wear debris, it was observed at 300°C that the wear mechanism was transformed from mild to severe wear due to the presence of laminated wear debris on the worn surfaces.
5. Overall, the fabricated nanocomposite with 0.25 wt.% GNP had promising wear performance, especially at elevated temperature, as a result of effective deagglomeration of GNP clusters. Therefore, these materials could be further developed and potential candidates to be utilized in the high temperature engineering applications subjected to substantial wear.

Acknowledgements

The Materials Research Center at İzmir Institute of Technology and Tallinn University of Technology are thanked for the use of their laboratory facilities.

Declaration of Conflicting Interests

The author(s) declared no potential conflicts of interest with respect to the research, authorship, and/or publication of this article.

Funding

The author(s) disclosed receipt of the following financial support for the research, authorship, and/or publication of this article: The present work was partially supported by "The Scientific and Technical Research Council of Turkey, TÜBİTAK" (Project No. 214M091). The authors acknowledge European Union Erasmus+ Mobility Programme for providing Mr. Seçkin Martin the opportunity to carry out the wear experiments at Tallinn University of Technology (Estonian Ministry of Education and Research SS427, M-ERA.NET Duracer ETAG 18012, PRG643).

ORCID iD

Sinan Kandemir https://orcid.org/0000-0001-6987-2737

References

1. Hirsch J. Aluminium in innovative light-weight car design. *Mater Trans* 2011; 52: 818–824.
2. Kim CS, Cho K, Manjili MH, et al. Mechanical performance of particulate-reinforced Al metal-matrix composites (MMCs) and Al metal-matrix nano-composites (MMNCs). *J Mater Sci* 2017; 52: 13319–13349.
3. Tjong SC. Recent progress in the development and properties of novel metal matrix nanocomposites reinforced with carbon nanotubes and graphene nanosheets. *Mater Sci Eng R Reports* 2013; 74: 281–350.
4. Donnet C and Erdemir A. Solid lubricant coatings: Recent developments and future trends. *Tribol Lett* 2004; 17: 389–397.
5. Donnet C and Erdemir A. Historical developments and new trends in tribological and solid lubricant coatings. *Surf Coatings Technol* 2004; 180-181: 76–84.
6. Miranda G, Buciumeanu M, Madeira S, et al. Hybrid composites - Metallic and ceramic reinforcements influence on mechanical and wear behavior. *Compos Part B Eng* 2015; 74: 153–165.
7. Akbari MK, Baharvandi H and Mirzaee O. Investigation of particle size and reinforcement content on mechanical properties and fracture behavior of A356-Al_2O_3 composite fabricated by vortex method. *J Compos Mater* 2014; 48: 3315–3330.
8. Ibrahim IA, Mohamed FA and Lavernia EJ. Particulate reinforced metal matrix composites – a review. *J Mater Sci* 1991; 26: 1137–1156.
9. Alipour M and Eslami-Farsani R. Synthesis and characterization of graphene nanoplatelets reinforced AA7068 matrix nanocomposites produced by liquid metallurgy route. *Mater Sci Eng A* 2017; 706: 71–82.
10. Dorri Moghadam A, Omrani E, Menezes PL, et al. Mechanical and tribological properties of self-lubricating metal matrix nanocomposites reinforced by carbon nanotubes (CNTs) and graphene – a review. *Compos Part B Eng* 2015; 77: 402–420.

11. Yang Y, Lan J and Li X. Study on bulk aluminum matrix nano-composite fabricated by ultrasonic dispersion of nano-sized SiC particles in molten aluminum alloy. *Mater Sci Eng A* 2004; 380: 378–383.
12. Hassan SF and Gupta M. Effect of nano-ZrO_2 particulates reinforcement on microstructure and mechanical behavior of solidification processed elemental Mg. *J Compos Mater* 2007; 41: 2533–2543.
13. Mazahery A, Abdizadeh H and Baharvandi HR. Development of high-performance A356/nano-Al_2O_3 composites. *Mater Sci Eng A* 2009; 518: 61–64.
14. Rashad M, Pan F, Tang A, et al. Improved strength and ductility of magnesium with addition of aluminum and graphene nanoplatelets (Al+GNPs) using semi powder metallurgy method. *J Ind Eng Chem* 2015; 23: 243–250.
15. Goh CS, Wei J, Lee LC, et al. Simultaneous enhancement in strength and ductility by reinforcing magnesium with carbon nanotubes. *Mater Sci Eng A* 2006; 423: 153–156.
16. Novoselov KS, Geim AK, Morozov SV, et al. Electric field effect in atomically thin carbon films. *Science* 2004; 306: 666–669.
17. Lee C, Wei X, Kysar JW, et al. Measurement of the elastic properties and intrinsic strength of monolayer graphene. *Science (80)* 2008; 321: 385–388.
18. Berman D, Erdemir A and Sumant AV. Graphene: a new emerging lubricant. *Mater Today* 2014; 17: 31–42.
19. Nieto A, Bisht A, Lahiri D, et al. Graphene reinforced metal and ceramic matrix composites: a review. *Int Mater Rev* 2017; 62: 241–302.
20. Baradaran S, Moghaddam E, Basirun WJ, et al. Mechanical properties and biomedical applications of a nanotube hydroxyapatite-reduced graphene oxide composite. *Carbon* 2014; 69: 32–45.
21. Hussainova I, Baronins J, Drozdova M, et al. Wear performance of hierarchically structured alumina reinforced by hybrid graphene encapsulated alumina nanofibers. *Wear* 2016; 368–369: 287–295.
22. Tabandeh-Khorshid M, Omrani E, Menezes PL, et al. Tribological performance of self-lubricating aluminum matrix nanocomposites: Role of graphene nanoplatelets. *Eng Sci Technol an Int J* 2016; 19: 463–469.
23. Turan ME, Sun Y, Akgul Y, et al. The effect of GNPs on wear and corrosion behaviors of pure magnesium. *J Alloys Compd* 2017; 724: 14–23.
24. Xiang SL, Gupta M, Wang XJ, et al. Enhanced overall strength and ductility of magnesium matrix composites by low content of graphene nanoplatelets. *Compos Part A Appl Sci Manuf* 2017; 100: 183–193.
25. El-Ghazaly A, Anis G and Salem HG. Effect of graphene addition on the mechanical and tribological behavior of nanostructured AA2124 self-lubricating metal matrix composite. *Compos Part A Appl Sci Manuf* 2017; 95: 325–336.
26. Abbasipour B, Niroumand B, Monir Vaghefi SM, et al. Tribological behavior of A356−CNT nanocomposites fabricated by various casting techniques. *Trans Nonferrous Met Soc China (English Ed* 2019; 29: 1993–2004.
27. Kandemir S. Effect of graphene nanoplatelets reinforcement on the microstructure and mechanical properties of AlSi10Mg alloy. *Gazi Üniversitesi Fen Bilim Derg Part C Tasarım ve Teknol* 2018; 6: 177–187.
28. Sharma A, Vasudevan B, Sujith R, et al. Effect of graphene nanoplatelets on the mechanical properties of aluminium metal matrix composite. *Mater Today Proc* 2019; 18: 2461–2467.
29. Dong HS and Qi SJ. Realising the potential of graphene-based materials for biosurfaces – a future perspective. *Biosurf Biotribol* 2015; 1: 229–248.
30. Lee JC, Byun JY, Park SB, et al. Prediction of Si contents to suppress the formation of Al_4C_3 in the SiC_p/Al composite. *Acta Mater* 1998; 46: 1771–1780.
31. Menezes PL, Nosonovsky M, Ingole SP, et al. *Tribology for scientists and engineers*. New York: Springer-Verlag, 2013.
32. Tian W, Li S, Wang B, et al. Graphene-reinforced aluminum matrix composites prepared by spark plasma sintering. *Int J Miner Metall Mater* 2016; 23: 723–729.
33. Alam SN and Kumar L. Mechanical properties of aluminium based metal matrix composites reinforced with graphite nanoplatelets. *Mater Sci Eng A* 2016; 667: 16–32.
34. Zafari A, Ghasemi HM and Mahmudi R. Tribological behavior of AZ91D magnesium alloy at elevated temperatures. *Wear* 2012; 292-293: 33–40.
35. Rajaram G, Kumaran S and Rao TS. High temperature tensile and wear behaviour of aluminum silicon alloy. *Mater Sci Eng A* 2010; 528: 247–253.
36. Jiang J, Stott FH and Stack MM. A generic model for dry sliding wear of metals at elevated temperatures. *Wear* 2004; 256: 973–985.
37. Cheng J, Li F, Qiao Z, et al. The role of oxidation and counterface in the high temperature tribological properties of TiAl intermetallics. *Mater Des* 2015; 84: 245–253.
38. Pauschnitz A, Roy M and Franek F. Mechanism of sliding wear of metals and alloys at elevated temperatures. *Tribol Int* 2011; 44: 584–602.
39. Antonov M and Hussainova I. Cermets surface transformation under erosive and abrasive wear. *Tribol Int* 2010; 43: 1566–1575.
40. Antonov M, Hussainova I and Adoberg E. Effect of loading system inertia on tribological behaviour of ceramic-ceramic, ceramic-metal and metal-metal dry sliding contacts. *Tribol Int* 2013; 65: 207–214.
41. Mengis L, Grimme C and Galetz MC. High-temperature sliding wear behaviour of an intermetallic γ-based TiAl alloy. *Wear* 2019; 426-427: 341–347.
42. Blau PJ. Elevated-temperature tribology of metallic materials. *Tribol Int* 2010; 43: 1203–1208.